UCRL--97539

DE88 003837

EMISSION OF γRAYS FROM VARIOUS MATERIALS PULSED WITH 14-MeV NEUTRONS

E. Goldberg, L. F. Hansen,
R. J. Howerton, T. T. Komoto,
and B. A. Pohl

This Paper was Prepared for Submittal to
Nuclear Explosives Design
Physics Conference
Los Alamos National Laboratory
October 19-23, 1987
Los Alamos, NM

October 1987

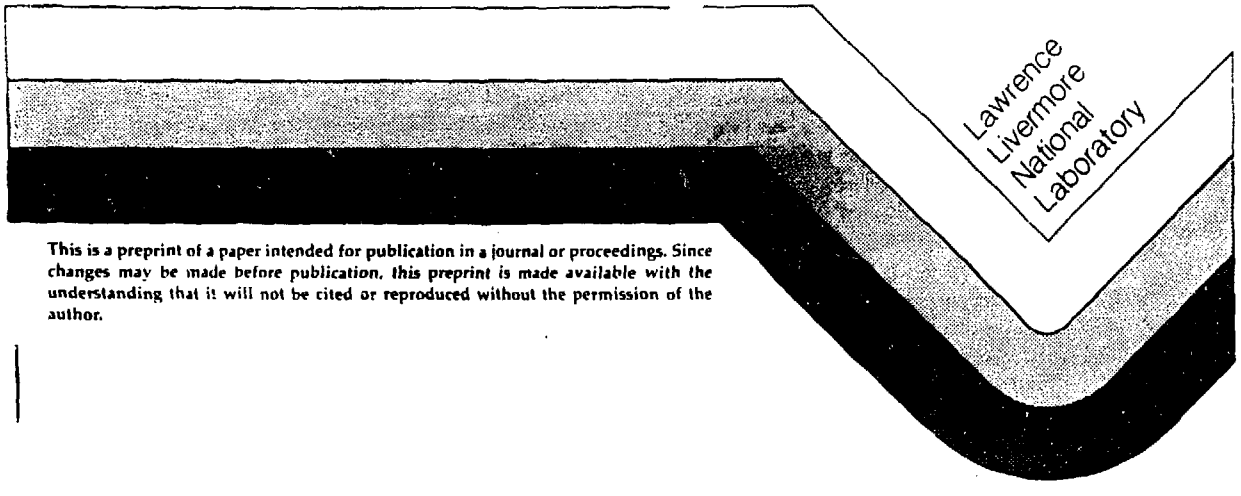

EMISSION OF γ RAYS FROM VARIOUS MATERIALS PULSED WITH 14-MeV NEUTRONS

E. Goldberg, L.F. Hansen, R.J. Howerton, T.T. Komoto, and B.A. Pohl

Lawrence Livermore National Laboratory

ABSTRACT

We have performed a number of experiments at LLNL recently to investigate the leakage of gamma rays from spheres of selected materials pulsed centrally with 14-MeV neutrons. Such spectral information may be carefully compared to calculational results to validate the transport models, particularly the nuclear cross section data base. In the present case, the TART code and SANDYL codes are used to explicitly calculate the observable, the recoil electron spectrum. The materials studied were H_2O, ^6LiD, Be, C, ^{14}N, CF_2, Al, Si, Ti, Fe, Cu, Ta, W, Au, Pb, Th, and ^{238}U. Generally, agreement was good between experiment and calculation. However, for some, the calculations significantly underestimated or overestimated experiment. For oxygen (i.e., H_2O), the ENDL cross section set led to a sizeable calculational overestimate. Re-examination led to a large improvement. For tungsten, the calculated output was ~30% below experiment. A re-evaluation led to closer agreement.

I. INTRODUCTION

As we explore advanced designs in nuclear weapons technology[1,2], the computational models employed often are found to be inadequate to the task, calling for a concerted effort to refine and certify the models. One procedure involves performance of integral experiments such as the pulsed sphere program[3] in which 14-MeV neutrons are generated as pulses at the center of a sphere of a particular material, and neutrons which leak from the sphere are timed to a distant detector. We report here an extension to that program, in which we performed a series of experiments at the RTNS-1 facility at LLNL to detect the gamma rays escaping the sphere. The procedure followed, which used for analysis the TART Monte Carlo code and the SANDYL photon-electron code, revealed in a number of experiments marked discrepancies between experiment and calculation. For a few of the more extreme cases, we undertook re-evaluations of the nuclear cross sections employed in TART.

These add to a large number of pulsed sphere experiments, the vast majority of which dealt with measurement of neutrons in flight enabling us to infer the neutron spectrum leaking from each sphere being studied. In the present instance, we measured signals caused by the escaping gamma rays as well as neutrons resulting from centrally-pulsed 14-MeV neutrons.

II. EXPERIMENTAL PROCEDURE

The experimental arrangement was chosen to have a geometry amenable to simple description in the model. The 14-MeV neutron source was housed in a low-mass structure and the spherical assembly slipped over the source so that the neutrons were manufactured in the central region of the assembly. The pulse rate of the 2-ns bursts of 400- keV deuterons was 500 kHz. The tritium loaded titanium target, 4 mg/cm^2 thick, was mounted at the end of the low-mass structure on a 0.76-cm-thick tungsten backing. Neutrons and gamma rays were detected by a single NE-213 scintillator detector, with electronics employing pulsed-shape discrimination to distinguish between neutrons and gamma rays. The center of the 5.1-cm-diameter, 5.1-cm-long detector was 852.5 cm from the neutron source. The spherical assembly, centered in one room, was visible to the detector in another room, through an iron collimator of 20.2 cm diameter mounted in a concrete wall of 197 cm thickness. The time window for acceptance of gamma ray-induced counts was 22 ns, while for neutrons, the time-of-flight was recorded for later analysis. A typical experiment was completed in a few hours.

We used our customary calibration procedure for the neutrons.[3] For the gamma rays, on the other hand, we had to perform an absolute calibration procedure utilizing sources

*This work was performed under the auspices of the U.S. Department of Energy by Lawrence Livermore National Laboratory under contract No. W-7405-Eng-48.

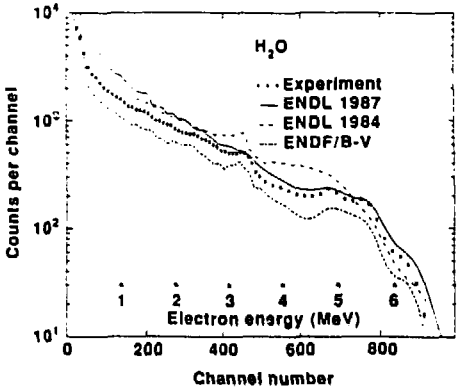

Fig. 1 Comparison of calculated to measured recoil electron spectra (RES) for a water-filled sphere.

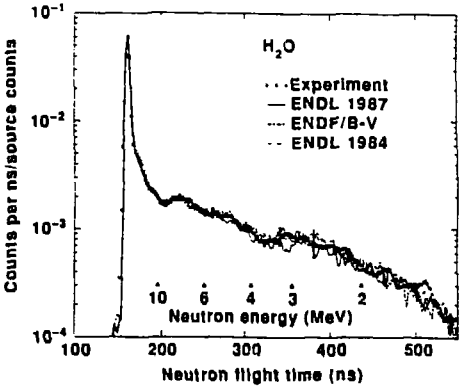

Fig. 2 Comparison of calculated to measured neutron time-of-flight (TOF) spectra for a water-filled sphere.

of ^{24}Na, ^{22}Na, ^{60}Co, and ^{137}Cs of known strength. Also, we were required to know the absolute neutron strength, which we did via use of a well-characterized proton-recoil counter. Through utilization of ^{238}Pu-^{13}C and ^{228}Th sources, we established detector linearity up to 6.13 MeV gamma ray energy. With a light pulser, we gathered evidence that linearity extended to 12 MeV.

III. CALCULATIONS

To properly compare the predictions of our computational model to experimental gamma ray-related results, the model must be capable of treating neutron and gamma ray generation and transport, and also electrons generated by the gamma rays that enter the NE-213 detector. The output of the Monte Carlo code, TART,[4] served as input to the gamma ray-electron transport code SANDYL.[5] Analysis of the neutron time-of-flight data is more straightforward since the neutron output spectrum associated with a particular spherical assembly is compared to the spectrum with sphere removed. What is needed in the analysis is the neutron energy-dependent detector response function which is folded into the TART-generated leakage spectrum to produce the counterpart to experimental observation.

Returning to the reaction gamma rays, we further note that the TART output is edited to exclude gamma rays that do not fall within the allowable time window, and also do not enter the collimator at an angle which implies a scatter subsequent to leakage from the sphere. All spheres investigated were within the field of view of the NE-213 detector.

Prior to analysis of the pulsed sphere experiments, we performed SANDYL calculations to compare to the gamma ray calibration experiments. Where the SANDYL code predicted sharp features to the recoil electron spectrum such as a Compton edge due to a monochromatic gamma ray component, we folded in a smoothing function, corresponding generally to 2-4% resolution. The ratio of calculated to experimental recoil electron spectrum for our first major series was 1.05 while for the second, we found a ratio of 1.09. We used these correction factors in our analysis.

IV. RESULTS

We have performed experiments using spherical assemblies of C, Al, Si, H_20, N, Ti, Fe, Cu, Be,^6LiD, Ta, W, Au, Pb, Th, ^{238}U, and C_2F_y. A general selection criterion was: $\rho\Delta r \sim 30$ gm/cm^2, since simple Monte Carlo calculations showed the gamma ray energy leakage was maximized for this value, leading to improved signal to background conditions. We will discuss five of these, of particular practical interest.

A. H_20

Bombardment of ^{16}O with 14-MeV neutrons gives rise to a number of energetic gamma rays, one prominent one being at 6.13 MeV. The medium employed was water contained in a spherical glass vessel, and escaping neutrons traveling forward along the beam axis passed through 14.5 gm/cm^2 of H_20 and 1.1 gm/cm^2 of pyrex glass. Our initial analysis revealed a large discrepancy with experiment, the calculated results exceeding experiment to a marked degree.

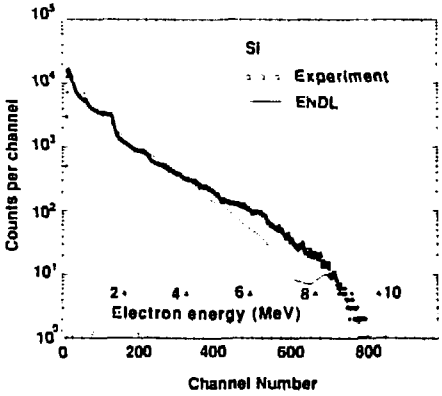

Fig. 3 Comparison of calculated to measured RES for silicon sphere.

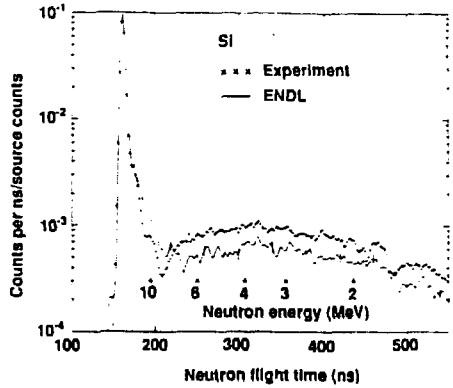

Fig. 4 Comparison of calculated to measured TOF spectra for silicon sphere.

On the other hand, when we employed ENDF/B-5 cross sections, calculated recoil electron spectra were one-half of measured values.[6]

Our most recent revision of the nuclear cross section data base for ^{16}O was incorporated into TART and Fig. 1 illustrates the calculated recoil electron spectrum (RES) compared to experiment. A measure of agreement takes the form:

$$\overline{C/E} = \frac{\sum C_i n_i (C/E)_i}{\sum C_i n_i}$$

where n_i is the number of experimental counts in channel C_i, and $(\overline{C/E})_i$ is the ratio of calculated to experimental counts in channel C_i. For the two runs, we found for $(\overline{C/E})$ values of 1.10 and 1.18, giving an average of 1.14. This is a considerable improvement over our initial comparison.[6] Our latest cross section re-evaluation accounts for the de-excitation of the 6.05 MeV level in ^{16}O via internal conversion. Figure 2, in which the neutron time-of-flight (TOF) spectra are compared, shows good agreement as it was before the cross sections were changed. For other materials as well, we found a number of instances where the neutron TOF spectrum was a weaker indicator of deficiencies in the cross section data base than the corresponding RES.

B. Silicon

We fabricated a spherical assembly of polycrystalline silicon of 10.16 cm radius, and $\rho\Delta r = 21.1$ gm/cm^2, and recorded its neutron and gamma ray leakage spectra generated by 14-MeV neutrons. Silicon was postulated, on the basis of preliminary calculations, to be a strong candidate as a gamma ray generator when irradiated by D-T neutrons. Using the standard ENDL cross section set,[7] we calculated the predicted RES. Figures 3 and 4 show the observed neutron TOF spectrum to disagree with the calculated spectrum, particularly for degraded neutrons. There the calculations are one-half the experimental values. For the gamma rays, we find, averaging over the experimental spectrum, $(\overline{C/E}) = 1.11$. Accordingly, silicon's nuclear cross section data base deserves close examination. The literature describes some careful measurements which exploit the existence of certain ^{28}Si (n,α) ^{25}Mg and ^{28}Si (n,p) ^{28}Al reactions.[8,9] These cross sections at E_n = 14 MeV are markedly smaller than those listed in the ENDL library. Table 1 lists another pertinent quantity,

$$\int \frac{d\sigma(n,x\gamma)}{dE_\gamma} \cdot E_\gamma dE_\gamma \equiv \overline{\sigma(n,x\gamma)E_\gamma}$$

We see for silicon a variation among measurements of ~50%. Our pulsed sphere experiment is compatible with a value of 6.3 barn-MeV.

C. Tungsten

The tungsten assembly was a spherical shell, 2.54 cm thick, with an outer radius of 10.36 cm. Figures 5 and 6 illustrate the RES, the neutron TOF spectrum, and the results of TART/SANDYL calculation. Along with ENDL-based results, we also employed the ENDF/B-5 cross section set.We see in the case of the RES, the early ENDL set led to a ~30% discrepancy, with calculation falling below

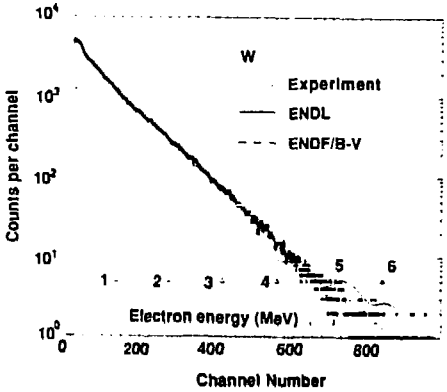

Fig. 5 The ENDL-based calculation utilized a 1984 data base.

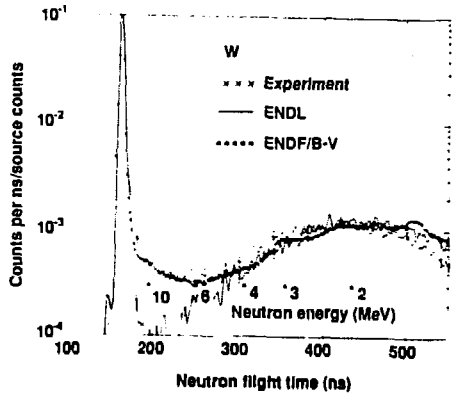

Fig. 6 The ENDL-based calculation utilized a 1984 data base.

postulated, on the basis of preliminary calculations, to be a strong candidate as a gamma ray generator when irradiated by D-T neutrons. Using the standard ENDL cross section set,[7] we calculated the predicted RES. Figures 3 and 4 show the observed neutron TOF spectrum to disagree with the calculated spectrum, particularly for degraded neutrons. There the calculations are one-half the experimental values. For the gamma rays, we find, averaging over the experimental spectrum, $(\bar{Q}_E) = 1.11$. Accordingly, silicon's nuclear cross section data base deserves close examination. The literature describes some careful measurements which exploit the existence of certain $^{28}Si\ (n,\alpha)\ ^{25}Mg$ and $^{28}Si\ (n,p)\ ^{28}Al$ reactions.[8,9] These cross sections at E_n = 14 MeV are markedly smaller than those listed in the ENDL library. Table 1 lists another pertinent quantity,

$$\int \frac{d\sigma(n,x\gamma)}{dE_\gamma} \cdot E_\gamma dE_\gamma \equiv \overline{\sigma(n,x\gamma)E_\gamma}$$

We see for silicon a variation among measurements of ~50%. Our pulsed sphere experiment is compatible with a value of 6.3 barn-MeV.

C. Tungsten

The tungsten assembly was a spherical shell, 2.54 cm thick, with an outer radius of 10.36 cm. Figures 5 and 6 illustrate the RES, the neutron TOF spectrum, and the results of TART/SANDYL calculation. Along with ENDL-based results, we also employed the ENDF/B-5 cross section set. We see in the case of the RES, the early ENDL set led to a ~30% discrepancy, with calculation falling below experiment. The discrepancy is even larger when the NDF/B-5 set is employed.

Table 1. Summary of $\overline{\sigma(n,x\gamma)E_\gamma}$

Element	ENDL[7]	ORNL[10]	Drake[11]	Bezotosnyi[12]	Rogers[14]
W	8.7[a] 9.9[b]	10.0		16.0	
Fe	9.1	10.2	6.8	10.2	
^{14}N	2.29	1.77			
C	1.02	0.80	1.00	1.13	
Si	7.0	4.7	4.5	7.2	4.3
Ti	6.6	8.4	6.7	10.5	
Al	6.3	4.3	4.1	5.7	
F	6.2[a] 1.8[b]	0.86		0.63[13]	
^{16}O	3.4[a] 3.1[b]	2.5			

[a] File: PP840818
[b] File: TG870815

We reviewed the literature and updated the ENDL data base. The calculational results, not shown in Figures 5 and 6, are somewhat closer to experiment, but a 20% discrepancy in RES still remains. The experimental values for $\overline{\sigma(n,x\gamma)E_\gamma}$ in Table 1 are quite far apart. Our experimental information is quite compatible with the Oak Ridge (ORNL-4847) findings.

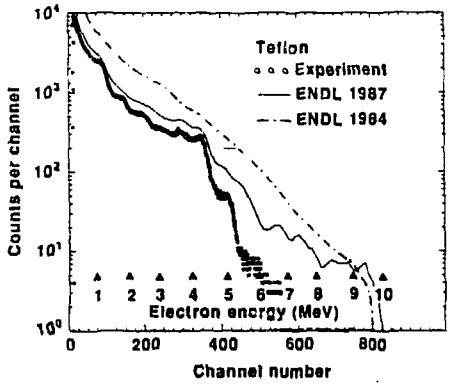

Fig. 7 Comparison of calculated to measured RES for teflon sphere.

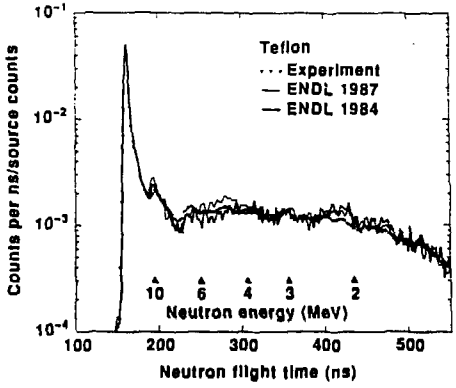

Fig. 8 Comparison of calculated to measured TOF spectra for teflon spherical shell.

D. Teflon (C_2F_4)

To study the gamma ray-generating character of fluorine, we employed a spherical shell of teflon (C_2F_4) with an outer radius of 16.5 cm and thickness of 35.2 gm/cm^2. Figures 7 and 8 illustrate the RES neutron TOF spectra resulting from the experiment and calculations. The calculated recoil spectrum exceeds experiment by a factor of four when the traditional cross section set is employed, while the calculated neutron TOF spectrum using the same data base agrees well with experiment. Re-evaluation of the fluorine cross sections led to a marked improvement in calculating the RES.

Table 1 shows the value of $\overline{\sigma E}$ for fluorine drawn from the ENDL set to be 6.2 barn-MeV, which greatly exceeds the experimental values of 0.86 and 0.63 barn-MeV. Upon re-evaluation, the ENDL value dropped to 1.8 barn-MeV. The RES derived from the newer ENDL set, shown on Figure 7, is much closer to experiment, but is still ~30% above. The newer set recognizes a much larger ^{4}He production cross section measured at E_n = 14 MeV.[15] In the newer ENDL set, the $^{19}F(n,n'\alpha)^{16}N$ reaction is the major mechanism for ^{4}He production. A crude argument points to a value of $\overline{\sigma E}$ of 1.2 barn-MeV at E_n = 14 MeV for fluorine, to reconcile with our experiment.

E. ^{14}N

In 1977, we reported on a series of experiments involving liquid nitrogen in which the gamma rays generated by 14-MeV neutrons were measured.[16] For that study, the electron transport was crudely approximated in the analysis. Accordingly, we selected from our vessels a spherical assembly for containing liquid nitrogen which maximized gamma ray leakage, and proceeded. Analysis involved TART/SANDYL.

A double-walled stainless steel dewar flask designed to accommodate liquid nitrogen out to a radius of 19.05 cm was employed. Along the beam axis, ($\rho\Delta R$) for ^{14}N was 14.76 gm/cm^2 and for the steel was 2.31 gm/cm^2. The geometry was closely modelled in TART. Figures 9 and 10 depict the RES neutron time-of-flight spectrum. We see excellent agreement between the measured and calculated RES, with a ratio of $(\overline{C/E})$ = 0.99.

We may infer from the values of $\overline{\sigma E}$ for ^{14}N in Table 1 that our pulsed sphere experiment favors $\overline{\sigma E}$ = 2.3 barn-MeV. However, the ORNL value is 1.77 barn-MeV (E_γ > .75 MeV) which compares poorly with the ENDL value (which when corrected to the same threshold drops to 2.23 barn-MeV). Additional careful microscopic cross section measurements on ^{14}N would help to clarify this matter.

V. CONCLUSIONS

We have performed a series of integral measurements in which outgoing neutrons and gamma rays generated in spherical assemblies of materials of interest by 14-MeV neutrons have been detected and their energy spectra examined. Careful analysis involving the TART and SANDYL Monte Carlo codes enable us to gain insight into the nature and quality of the nuclear cross section

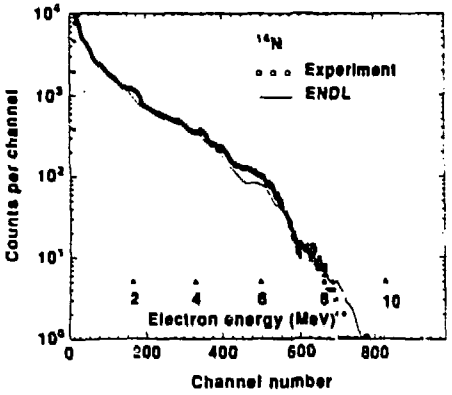

Fig. 9 Comparison of calculated to measured RES for nitrogen-filled vessel.

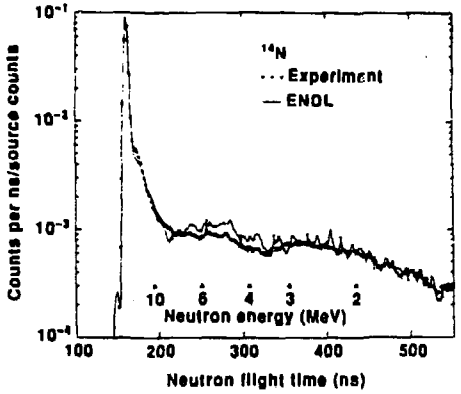

Fig. 10 Comparison of calculated to measured TOF spectra for nitrogen-filled spherical vessel.

information incorporated in the data bases employed. No clear trend is visible. In some instances like the tungsten study, we find the TART code underpredicting gamma ray emission. For the experiment involving H_2O, we find that TART overpredicts experiment when the ENDL set is used, but when the ENDF/B-5 set is used, under-prediction results.

For circumstances where 14-MeV neutrons play a major role, we find microscopic cross section data concerned with neutron-induced gamma rays to be relatively sparse, with uncertainties in the 15% range, and where experiments can be compared, disagreements well in excess of this figure abound. We strongly encourage careful microscopic measurements, with emphasis in the 14-MeV neutron range, aiming for 5-10% accuracy.

It is also clear that a number of cross section files are not up to date and deserve attention, particularly in their application to gamma ray production.

The pulsed sphere experimental program discussed here has proven to be an economical catalyst in the process certification of accuracy of our major nuclear radiation transport code, TART.

VI. REFERENCES

1. Reference deleted

2. Reference deleted

3. C. Wong, J.D. Anderson, P. Brown, L.F. Hansen, J.L. Kammerdiener, C. Logan, and B. Pohl, "Livermore Pulsed Sphere Program: Program Summary through July 1971," UCRL-51144, Rev. 1 (Feb. 10, 1972).

4. E.F. Plechaty and J.R. Kimlinger, "TARTNP: A Coupled Neutron-Photon Monte Carlo Transport Code," UCRL-50400 Vol. 14, (1976). The present name of this code is TART.

5. H.M. Colbert, "SANDYL, a Computer Program for Calculating Combined Photon-Electron Transport in Complex Systems," SLL-74-0012, (1974).

6. E. Goldberg, L.F. Hansen, R.J. Howerton, T.T. Komoto, and B.A. Pohl, "Neutron and Gamma Ray Emission from the Transport of 14 MeV Neutrons through H_2O," UCID-21064, LLNL, June 1987.

7. "ENDL," Lawrence Livermore National Laboratory (LLNL) Evaluated Nuclear Data Library, Evaluated by E.J. Howerton et al., UCRL-50400, Vol. 15, Parts A to E (1975-1978).

8. R.G. Miller and R.W. Kavanagh, Nucl. Instrum. Methods, 48, 13 (1967).

9. D.W. Mingay, J.P.F. Sellschop, and P.M. Johnson, Nucl. Instrum. Methods, 94, 497 (1971).

10. Series of ORNL reports: W(ORNL-4847), Fe(ORNL-TM-5416), ^{14}N(ORNL-4864), C(ORNL-TM-3702), Si(ORNL-TM-4389), Ti(ORNL-TM-6323), Al(ORNL-TM-4232), F(ORNL-TM-4538), and ^{16}O(ORNL-5575 Special).

11. D.M. Drake, E.D. Arthur, and M.G. Silbert, Nucl. Sci. Eng., 65, 49 (1977).

12. V.M. Bezotosnyi, V.M. Gorbachev, M.S. Shvetsov, and L.M. Surov, Atomnaya Energiya, 49, 239, (1980).

13. G.N. Maslov, F. Nasyrov, and N.F. Pashkin, Atomnaya Energiya, 24, 573 (1965).

14. V.C. Rogers et al., "Gamma Ray Production Cross Sections for Silicon and Copper from Threshold to 20-MeV," DNA 3818F (2 Oct. 1975).

15. D.W. Kneff, B.M. Oliver, H. Farrar IV, and L.R. Greenwood, Nucl. Sci. Eng. 92, 491 (1986).

16. L.F. Hansen, T.T. Komoto, E.F. Plechaty, B.A. Pohl, G.S. Sidhu, and C. Wong, Nucl. Sci. Eng. 62, 550 (1977).

DISCLAIMER